

PROPERTIES OF A NOISE BARRIER WITH CONTROLLED DIFFRACTION AT THE EDGE

V.T. GRINCHENKO¹, I.V. VOVK¹, V.O. HUSAK^{2*},
V.T. MATSYPURA²

¹*Institute of Hydromechanics of NAS Ukraine,
National Academy of Sciences of Ukraine, Kyiv, 01030, Ukraine*

²*Faculty of Mechanics and Mathematics,
Taras Shevchenko National University of Kyiv, Kyiv, 01033, Ukraine*

[Received: 28 March 2022. Accepted: 17 October 2022]

doi: <https://doi.org/10.55787/jtams.23.53.2.152>

ABSTRACT: The paper considers the problem of sound scattering on a classical noise barrier and a noise barrier with a resonator. A rigorous solution is obtained. It is shown that the use of the root mean square approximation and the conjugation by points of fields in the problem of sound scattering on a classical barrier gives a good coincidence of the calculated values of fields. It is shown that for frequencies above the resonance one exists a band in which there is a dip in the frequency response of the integral criterion of the barrier. All this illustrates the advantage of the barrier with the resonator.

KEY WORDS: noise barrier, diffraction, sound field, partial domains method (PDM), conjugation by points (CBP).

1 INTRODUCTION

The article investigates the possibility of using the CBP of sound fields in the PDM when solving the boundary-value problem (BVP) for the noncanonical domain of sound field existence [1, 2]. The problem of sound diffraction on a barrier with a resonator which is located at the edge of the barrier is considered. A rigorous solution is obtained that allows us to analyze the sound fields scattered by barriers in the frequency range of interest from a practical point of view.

Currently, much attention is paid to scientific programs aimed at studying noise pollution in cities and developing measures to reduce it [3–5]. Particular attention is paid to the method of noise reduction using barriers (acoustic screens) placed between the noise sources and the area to be protected from its effects (residential buildings,

*Corresponding author e-mail: gusakw7@gmail.com

sidewalks near highways, workplaces in manufacturing). The reason for the popularity of barriers is due to their relative cheapness and ease of use.

The noise protection effect of the described barriers is reduced to the effect of acoustic shielding, i.e. creating a sound shadow zone around the protected object. Most of the publications devoted to estimations of sound fields scattered by barriers are based on the use of approximate approaches, in particular methods of ray acoustics, Keller, and other asymptotic methods [6, 7]. These methods make it possible to obtain good estimates of the fields behind the barrier (in the domain of its acoustic shadow) for cases where the height of the barrier significantly exceeds the length of the sound wave incident on it.

It is possible to distinguish a series of articles, in which the noise protection properties of barriers with built-in structures in the form of resonators are investigated [8–13]. These studies were carried out based on numerical methods.

In most practical cases, most of the sound energy of traffic and industrial noise lies in the domain of relatively low frequencies. The maximum of the noise energy is in the domain of 50–200 Hz [14], which corresponds to a wavelength of 1.5–6 m.

The actual height of noise barriers erected near traffic arteries varies from 3 to 6 m. When studying sound scattering on bodies comparable to the sound wavelength, it is necessary to use rigorous methods when setting and solving the corresponding diffraction problems. Otherwise, the results of estimates of the scattered field may turn out to be far from the truth. The paper describes a rigorous solution to the problem of sound scattering on a barrier with a resonator that is located at the edge of the barrier.

2 CLASSIC BARRIER

First, let us consider the classic barrier model. Let us make sure that two approaches to the conjugation of fields on the boundaries of partial domains (PD) are possible when solving the problem by the PDM, namely:

- the root mean square approximation (RMS) of fields,
- the CBP of fields (let's call these points nodal).

2.1 MATHEMATICAL MODEL OF THE BARRIER

Classic barrier is a solid vertical wall of rigid material, the height of which is much greater than its thickness. Barriers are installed on the sides of highways in the form of a continuous wall, the length of which is much greater than its height. Let's assume that the traffic flow is dense and sufficiently intense (more than two thousand vehicles per hour). In this case, the intensity of the noise generated by the flow is virtually independent of the magnitude of the contribution of the individual transport unit.

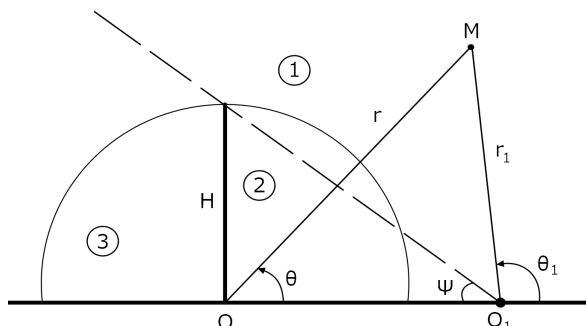


Fig. 1: Geometry of the classic barrier model.

Let's consider the mathematical model of the classical barrier located along the transport highway (Fig. 1). Let's assume that on an infinite acoustically rigid surface, which models the surface of the Earth, an infinite (along the direction perpendicular to the plane of the figure) acoustically rigid thin barrier of height H is placed at point O . To the right, parallel to the barrier at a point O_1 , there is a linear harmonic sound source with frequency ω in the form of an infinitely long pulsating thread (simulates the noise created by the traffic flow). Point O_1 is located on an acoustically rigid surface at a distance $OO_1 = r_S$ from point O . The letter M marks the observation point. The entire half-space is filled with an ideal acoustic medium with the density ρ and speed of sound c , which correspond to the parameters of the air medium.

The described model is equivalent to the plane problem from the point of view of mathematics in which the parameters of the sound field do not depend on one of the coordinates. In our case, the coordinates perpendicular to the plane of the figure. The accepted acoustic properties of the earth's surface and barrier mean that the normal component of the vibrational velocity of the sound field on them is zero.

2.2 CONSTRUCTING AN ANALYTICAL SOLUTION

Let's introduce a polar coordinate system (r, θ) with the center at a point O (Fig. 1). The entire space of existence of the sound field is divided into three domains: domain 1 is a semicircle of radius H , i.e. $r \geq H, 0 \leq \theta \leq \pi$; domain 2 is a right sector of a semicircle of radius $H : r \leq H, 0 \leq \theta \leq \pi/2$; domain 3 is a left sector of a semicircle: $r \leq H, \pi/2 \leq \theta \leq \pi$.

The described separation of PD is directly related to the way the BVP is constructed. It is for such domains that a general solution of the Helmholtz equation can be constructed. Wherein the solution of the initial BVP is reduced to the fulfillment of conjugation conditions on the boundaries of PD. We do not write the multiplier $\exp(-i\omega t)$ everywhere.

Let us place the center O_1 of the second polar coordinate system (r_1, θ_1) at the source location, Fig. 1. Let us assume the source is located in domain 1, that is, $r_S > H$. Let us represent the pressure field of a linear source as $p_S(r_1, \theta_1) \equiv p_S(r_1) = H_0^{(1)}(kr_1)$, where $H_0^{(1)}(kr_1)$ is a Hankel function of the first kind of zero order, $k = \omega/c$ is the wave number, $\omega = 2\pi f$, f is the frequency.

The pressure field in domain 1 is

$$(1) \quad p_1 = \sum_{n=0}^{\infty} A_n^{(1)} \frac{H_n^{(1)}(kr)}{H_n^{(1)'}(kH)} \cos(n\theta) + p_S(r_1, \theta_1).$$

The hatch in the Hankel function means the derivative on the argument.

Let us represent the pressure field in domain 2 as a superposition of standing waves

$$(2) \quad p_2 = \sum_{n=0}^{\infty} A_n^{(2)} \frac{J_{2n}(kr)}{J_{2n}'(kH)} \cos(2n\theta).$$

Similarly, for domain 3, the pressure field is

$$(3) \quad p_3 = \sum_{n=0}^{\infty} A_n^{(3)} \frac{J_{2n}(kr)}{J_{2n}'(kH)} \cos\left(2n\left(\theta - \frac{\pi}{2}\right)\right).$$

In formulas (1)–(3) standard notations for Bessel and Hankel functions are adopted.

The conjugation conditions of the fields at the boundary of PD 1 and 2, 3 have the form

$$(4) \quad p_1 = p_2, \quad r = H, \quad \theta = \left[0, \frac{\pi}{2}\right],$$

$$(5) \quad p_1 = p_3, \quad r = H, \quad \theta = \left[\frac{\pi}{2}, \pi\right],$$

$$(6) \quad \frac{\partial p_1}{\partial r} = \begin{cases} \frac{\partial p_2}{\partial r}, & r = H, \quad \theta = \left[0, \frac{\pi}{2}\right] \\ \frac{\partial p_3}{\partial r}, & r = H, \quad \theta = \left[\frac{\pi}{2}, \pi\right]. \end{cases}$$

Substituting the expressions for the fields in the PD (1)–(3) into the conjugation conditions of the fields (4)–(6), we obtain an infinite system of equations that contains functions of the angular coordinate θ .

The transition from the resulting equations to an infinite system of linear algebraic equations can be done in two ways:

- the first, by applying the RMS approximation when the boundary conditions are satisfied,

- the second – using the CBP of the fields at the boundary.

We will solve the infinite system of linear algebraic equations by the method of reduction, controlling the quality of fulfillment of the boundary conditions in the course of calculations. For this purpose let us restrict the infinite series in expressions (1)–(3) by setting the number of coefficients $A_n^{(1)}$, $A_n^{(2)}$, $A_n^{(3)}$ respectively N_1 , N_2 , N_3 . Let us assume that $N_2 = N_3 = N_1/2$.

THE RMS APPROXIMATION

In this approach, we multiply scalarly: expression (4) by the functions $\cos(2m\theta)$, $m = 0, 1, 2, \dots, N_2$; expression (5)– by the functions $\cos(2m(\theta - \pi/2))$, $m = 0, 1, 2, \dots, N_3$; and expression (6) by the functions $\cos(m\theta)$, $m = 0, 1, 2, \dots, N_1$. We use the orthogonality property of the given sets of trigonometric functions on the intervals specified in the conjugation conditions of the fields (4)–(6).

As a result, we come to a system of linear algebraic equations of the second kind, the order of which is determined by the number of taken into account coefficients $A_n^{(1)}$, $A_n^{(2)}$, $A_n^{(3)}$, namely $N_1 + N_2 + N_3$.

THE CBP OF FIELDS ON THE BOUNDARY

Let us denote the coordinates of conjugation points (nodal points) at the interface of PD 1 and 2, 3 – $(r_m = H, \theta_m)$, $m = 0, 1, 2, \dots, N_1$. Choosing angular coordinates of nodal points $0 < \theta_m < \pi$, $m = 0, 1, 2, \dots, N_1$ we write expressions (4)–(6) as a system of linear algebraic equations of the order $N_1 + N_2 + N_3$.

2.3 ANALYSIS OF NUMERICAL RESULTS

The analytical representations of the sound field constructed within the PDM always exactly satisfy the wave equation for any number of terms held in the series. Therefore, on the basis of accurate estimates of the solution of the problem as a whole one should put an estimate of the execution accuracy of the conjugation conditions on the boundaries of PD. To increase the accuracy of the estimation of the sound fields scattered by the barrier, it is necessary to increase the number of unknown complex coefficients when solving the algebraic system of equations by the reduction method.

Note that the efficiency of algorithms for solving infinite systems of algebraic equations can be ensured by taking into account the known singularities in the neighborhood of corner points. In our case it is the top edge of the barrier. This makes it possible to obtain quantitative estimates of the characteristic of the sound fields in domains close to the corner points. If, however, the main interest is the characteristics of the field at points distant from the angular ones, then, sufficient accuracy of the results can be ensured by using the method of simple reduction, keeping a cer-

tain number of equations in the system. Numerical experiments were carried out to evaluate the degree to which the conditions for the conjugation of the sound fields for the selected range of frequency values were met. Such a procedure is standard when using the PDM and has been tested by us more than once.

Let us focus our attention on the comparison of the two approaches noted above when the field conjugation conditions at the boundaries of PD are satisfied.

As integral characteristics of acoustic properties of noise barriers, it is advisable to use the energy characteristics of the sound field, such as the total power emitted by the source W_0 (naturally in the presence of the barrier) and the power of the sound field W_D penetrating into the geometric shadow zone of the barrier due to diffraction [2]. Figure 1 schematically shows the barrier with all the parameters necessary to find the angle of opening of the geometric shadow ψ .

As an integral spatial criterion for evaluating the noise protection properties of the barrier we choose the value $G = W_D/W_0$, which, in its essence, is the energy coefficient of sound penetration into the shadow zone of the barrier.

The calculation of the average power per period of the source per unit of its length can be done by integrating over the arc of the half-circle of the radius r in the far zone of the radiating system source-barrier

$$W_0 = \int_0^{\pi} I(r, \theta) r d\theta, \quad W_D = \int_{\pi-\psi}^{\pi} I(r, \theta) r d\theta,$$

where the intensity $I = |p|^2 / (2\rho c)$.

The starting point in the calculations for the CBP of the fields is normalized to the wavelength $\lambda = c/f$ distance between the nodal points $\Delta h/\lambda$ along the interface of PD 1 and 2, 3, that is, the value $\Delta h/\lambda$. Based on the $\Delta h/\lambda$ value, the number of nodal points $N_1 = [L/\Delta h]$, $L = \pi H$; $N_2 = N_3 = N_1/2$.

It is now necessary to establish the relation between the calculations performed using the CBP of the fields and the RMS approximation. To do this, when using the RMS approximation, the number of modes in domain 1 is set to N_1 , the number of modes in domain 2 is set to N_2 , and in domain 3, N_3 . In this case, the order of the systems of equations for the two variants of conjugate fields will be the same, namely $N_1 + N_2 + N_3$.

Let the parameters of the classical barrier model be as follows: barrier height $H = 4$ m, distance to the sound source $r_S = 6$ m, the geometric shadow zone are determined by the range of angle change $\theta = [\pi - \psi, \pi]$, under these problem conditions $\psi \approx 34^\circ$.

As the calculations show, the wave distance between the nodal points should be chosen according to the inequality $\Delta h/\lambda \leq 0.15$. Let $\Delta h/\lambda = 0.05$. Then the

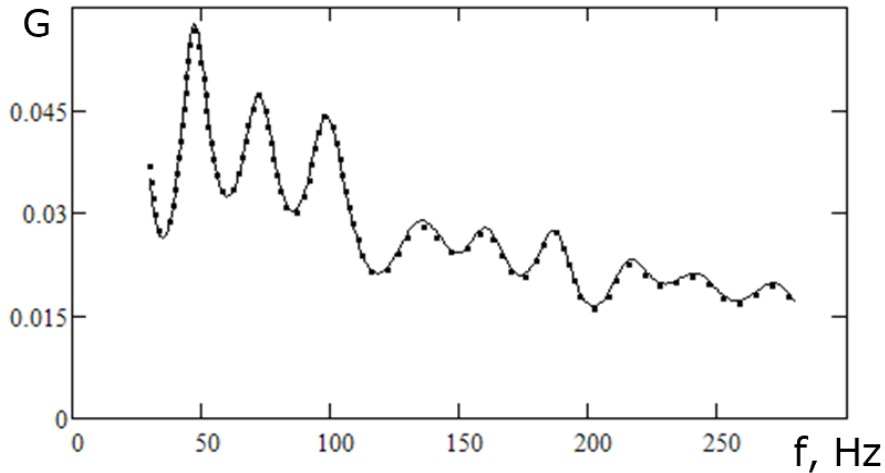


Fig. 2: Classical barrier. Frequency dependence of the energy coefficient of sound transmission into the shadow zone of the barrier $G(f)$, $H = 4$ m, $r_S = 6$ m, $\psi \approx 34^\circ$, $\Delta h/\lambda = 0.05$, $N_1 = 24 \dots 208$: line – the CBP, points – the RMS approximation.

number N_1 of nodal points at the interface of PD 1 and 2, 3 (half circle of radius H), when changing the frequency f from 30 Hz to 280 Hz, changes linearly from the value of $N_1 = 24$ to $N_1 = 208$. Correspondingly, when the RMS approximation, the number of modes in domain 1 also changes.

Figure 2 shows the frequency dependence of the energy coefficient of sound transmission into the shadow zone of the barrier $G(f)$. Analyzing the graphs in Fig. 2, we note a good coincidence of the calculated data for the two cases of conjugation of the fields at the boundary of PD in the entire frequency range. The efficiency of the classical barrier decreases in the low frequency range, remaining almost constant at frequencies above 300 Hz.

In the range of model parameters of interest to us, there is good (with graphic accuracy) conjugation of the fields in both variants of the calculation. In this case, there is a coincidence between the calculated values of the fields for the CBP of fields and in the RMS. Of course, there is a peculiarity in the behavior of the velocity in the vicinity of the corner point (the upper edge of the barrier), which is a quite predictable result.

3 BARRIER WITH THE RESONATOR

The sound field in the geometric shadow domain for the classical barrier (Fig. 1) is determined by the rays scattered on the barrier edge. It is these rays that are the

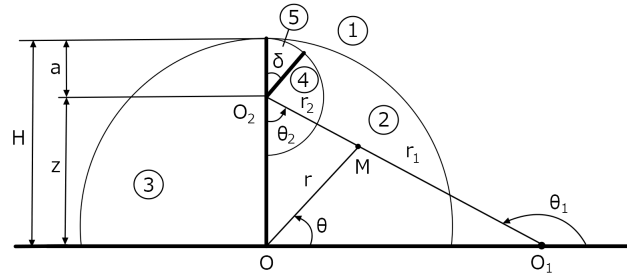


Fig. 3: Geometry of the barrier model with the resonator (domain 5).

main cause of the sound field in the shadow zone behind the barrier. Thus, if it were possible to attenuate the intensity of the rays scattered at the edge of the barrier, it would be possible to reduce the sound field in the shadow zone behind the barrier. This will increase its efficiency without having to increase the height of the barrier.

To implement this idea, we place a resonator at the edge of the barrier in the form of a sector with rigid walls (Fig. 3). Due to the interference of waves inside the resonator, a standing wave is formed along its axis. If the parameters of the resonator are properly sized, the maximum sound pressure domain is set at the bottom of the resonator. And at the resonator inlet the minimum sound pressure domain is set. Accordingly, the level of sound "flowing" over the barrier should decrease.

3.1 CONSTRUCTING AN ANALYTICAL SOLUTION

The geometry of the barrier model with the resonator is shown in Fig. 3. The resonator is a circular sector with an opening angle δ and sides of length a (domain 5). We assume that all surfaces of the barrier are perfectly rigid. To construct a solution to this problem, in addition to the two polar coordinate systems (r, θ) and (r_1, θ_1) , we introduce a third polar coordinate system (r_2, θ_2) centered at the point O_2 (Fig. 3). The entire space of sound field existence is divided into five domains:

- domain 1 is a semicircle of radius H , i.e. $r \geq H, 0 \leq \theta \leq \pi$;
- domain 2 is a right sector of a semicircle of radius H : $r \leq H, 0 \leq \theta \leq \pi/2$ minus the semicircle of radius a : $r_2 \leq a, 0 \leq \theta_2 \leq \pi$;
- domain 3 is a left sector of a semicircle: $r \leq H, \pi/2 \leq \theta \leq \pi$;
- domain 4 is a sector: $r_2 \leq a, 0 \leq \theta_2 \leq \pi - \delta$;
- domain 5 is a sector: $r_2 \leq a, \pi - \delta \leq \theta_2 \leq \pi$.

We write the fields in the PD (Fig. 3) in the form

$$(7) \quad p_1 = \sum_{n=0}^{\infty} A_n^{(1)} \frac{H_n^{(1)}(kr)}{H_n^{(1)'}(kH)} \cos(n\theta) + p_S(r_1, \theta_1),$$

$$(8) \quad p_2 = \sum_{n=0}^{\infty} A_n^{(2)} \frac{J_{2n}(kr)}{J'_{2n}(kH)} \cos(2n\theta) + \sum_{n=0}^{\infty} A_n^{(2)} \frac{H_n^{(1)}(kr_2)}{H_n^{(1)'}(ka)} \cos(n\theta_2),$$

$$(9) \quad p_3 = \sum_{n=0}^{\infty} A_n^{(3)} \frac{J_{2n}(kr)}{J'_{2n}(kH)} \cos\left(2n\left(\theta - \frac{\pi}{2}\right)\right),$$

$$(10) \quad p_4 = \sum_{n=0}^{\infty} A_n^{(4)} \frac{J_{\alpha_n}(kr_2)}{J'_{\alpha_n}(ka)} \cos(\alpha_n \theta_2), \quad \alpha_n = \frac{n\pi}{\pi - \delta},$$

$$(11) \quad p_5 = \sum_{n=0}^{\infty} A_n^{(5)} \frac{J_{\beta_n}(kr_2)}{J'_{\beta_n}(ka)} \cos(\beta_n (\theta_2 - (\pi - \delta))), \quad \beta_n = \frac{n\pi}{\delta}.$$

Let us write down the conjugation conditions for the fields

$$(12) \quad p_1 = p_2, \quad r = H, \quad \theta = [0, \pi/2],$$

$$(13) \quad p_1 = p_3, \quad r = H, \quad \theta = [\pi/2, \pi],$$

$$(14) \quad \frac{\partial p_1}{\partial r} = \begin{cases} \frac{\partial p_2}{\partial r}, & r = H, \quad \theta = [0, \pi/2], \\ \frac{\partial p_3}{\partial r}, & r = H, \quad \theta = [\pi/2, \pi], \end{cases}$$

$$(15) \quad \frac{\partial p_2}{\partial r_2} = \begin{cases} \frac{\partial p_4}{\partial r_2}, & r_2 = a, \quad \theta_2 = [0, \pi - \delta], \\ \frac{\partial p_5}{\partial r_2}, & r_2 = a, \quad \theta_2 = [\pi - \delta, \pi], \end{cases}$$

$$(16) \quad p_2 = p_4, \quad r_2 = a, \quad \theta_2 = [0, \pi - \delta],$$

$$(17) \quad p_2 = p_5, \quad r_2 = a, \quad \theta_2 = [\pi - \delta, \pi].$$

Substituting expressions (7)–(11) into conditions (12)–(17), we obtain an infinite system of equations. This system contains angular functions at certain intervals of change in angular coordinates θ , θ_1 and θ_2 . The transition to a finite system of linear algebraic equations of the second kind is performed based on the CBP of the fields at the interfaces of PD. Given the rather complex partitioning of the field's existence domain into PD and the presence of three polar coordinate systems (Fig. 3), we can argue that using the CBP of the fields, as compared with the RMS approximation, will significantly simplify the amount of analytical and computational work.

Parameters of the resonator are determined from the following considerations:

- we find the value a from the first resonance condition for PD 5 under the conditions of rigid walls of domain 5 and zero pressure on the arc $r_2 = a$, $\theta_2 = [\pi - \delta, \pi]$. According to the above boundary conditions, the desired value a is the root of the equation $J_0(2\pi a/\lambda) = 0$. Hence $2\pi a/\lambda = 0.7655\pi$ and $a = 0.38275\lambda$;
- the optimum value of width of the resonator opening is approximately equal to 0.2λ , that is $a\delta = 0.2\lambda$. Substituting in this relation expression $a = 0,38275\lambda$, we find the value of angle $\delta = 30^\circ$.

3.2 ANALYSIS OF NUMERICAL RESULTS

In the beginning, we present typical graphs that illustrate the quality of fulfillment of the field conjugation. As an example, Fig. 4 shows the fields at the interface of PD 1 and 2, 3. Model parameters: $H = 4$ m, $r_S = 6$ m, $\psi \approx 34^\circ$, $\Delta h/\lambda = 0.05$, the resonant frequency of the resonator $f_{\text{rez}} = 100$ Hz, the geometric parameters of the resonator are as follows: $a = 1.3$ m, $\delta = 30^\circ$. The number of nodal points at the interface of PD 2 and 4, 5 increased by a factor of four or six. According to the selected parameters, the number of nodal points was as follows: on the boundary of PD 1 and 2, 3 — 76, on the boundary of domain 4 — 82, on the boundary of domains 5 — 16. With a relatively small number of nodal points, and hence the number of modes considered in PD, we obtained a good coincidence of the fields on the boundaries of PD.

As an integral energy criterion of the barrier with the resonator let's take the ratio of sound field powers penetrating into the geometric shadow zone of the barrier with

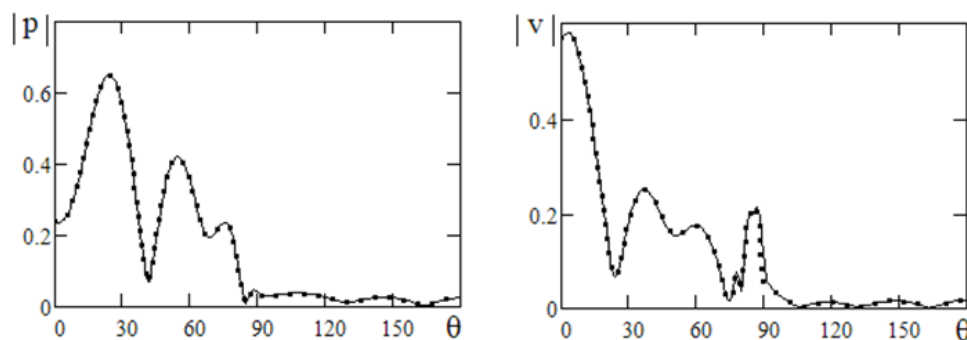


Fig. 4: Barrier with the resonator, modules of pressure $|p|$ and normal vibrational velocity $|v|$ at the boundaries of PD 1 and 2, 3; $H = 4$ m, $r_S = 6$ m, $f = f_{\text{rez}} = 100$ Hz; $\Delta h/\lambda = 0.05$: lines – field on the side of domain 1; points – field on the side of domains 2 and 3.

the resonator W_{Db} and the classical barrier W_D : $G_b = W_{Db}/W_D$.

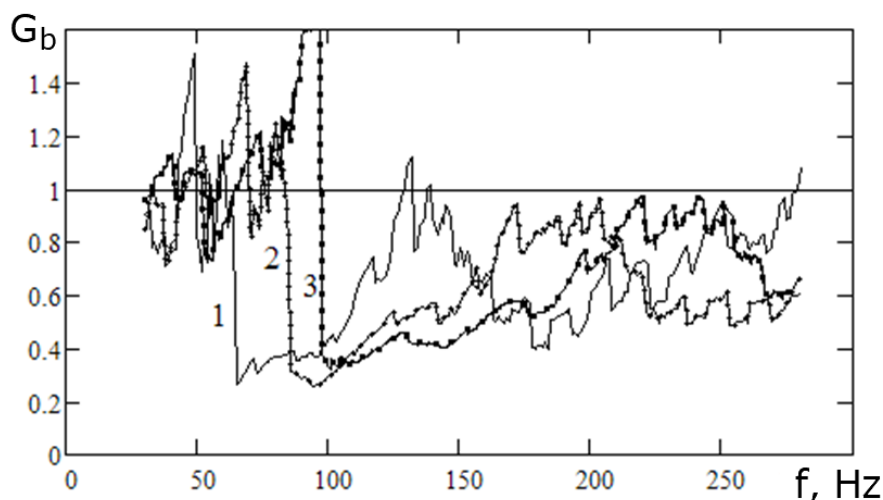


Fig. 5: Frequency dependencies of the integral criterion of the barrier $G_b(f)$, $H = 4$ m, $r_S = 6$ m, $\psi \approx 34^\circ$: 1 — $f_{\text{rez}} = 75$ Hz, 2 — $f_{\text{rez}} = 100$ Hz, 3 — $f_{\text{rez}} = 125$ Hz.

Figure 5 shows the frequency dependences of the integral criterion of the barrier $G_b(f)$. In the calculated frequency range from 30 Hz to 280 Hz, the number of nodal points on the interface of PD 1 and 2, 3 changed according to a linear law from 12 to 112. The number of nodal points on the boundary of domain 5 changed according to a linear law from 4 to 36. The parameter of the curves is the resonance frequency of the resonator: curve 1 — $f_{\text{rez}} = 75$ Hz, 2 — $f_{\text{rez}} = 100$ Hz, 3 — $f_{\text{rez}} = 125$ Hz. The geometric size of the resonator changes accordingly, namely the values $a = 1.7, 1.3, 1.0$ m.

For all three variants of calculation we can distinguish common features in the behavior of the frequency characteristics:

- the value of the integral criterion of the barrier $G_b(f)$ near the resonant frequency is approximately the same for the three resonator variants and is 0.3;
- for frequencies above the resonant frequency, there is a frequency band in which there is a dip in the frequency response $G_b(f)$. This indicates the advantage of the barrier with the resonator. As the resonant frequency increases, this frequency band increases;
- at frequencies above these bands we have a value of $G_b(f) < 1$, although gradually the efficiency of the barrier with the resonator and the classical barrier is

getting closer;

- at frequencies below resonance, there are situations in which the efficiency of a barrier with a resonator is worse than that of a classical barrier.

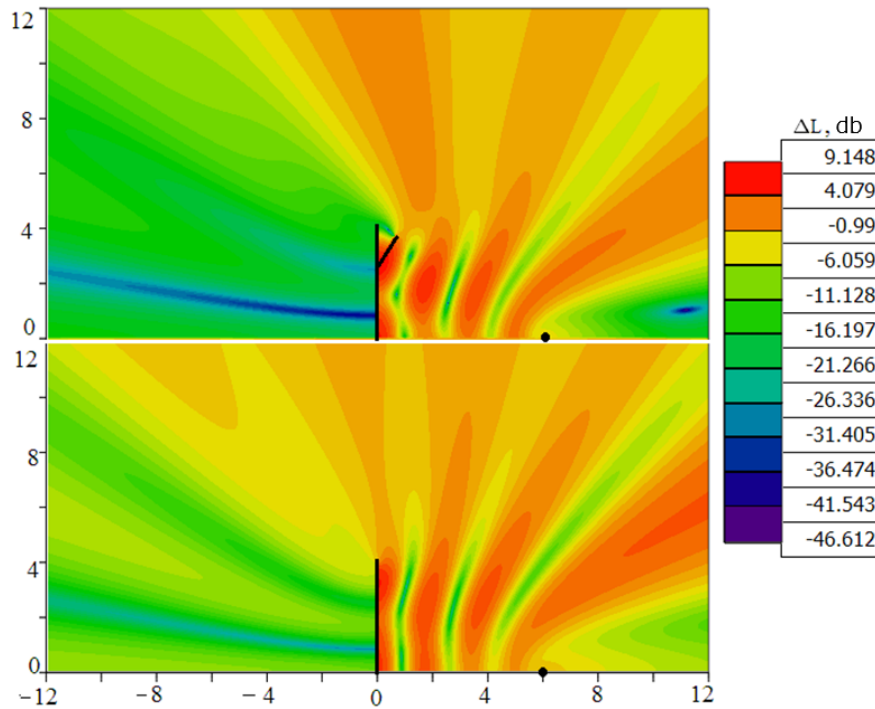


Fig. 6: Distribution of ΔL in the vicinity of the barrier (coordinates are in meters, the black dot is the source), $H = 4$ m, $r_S = 6$ m, $f = f_{rez} = 100$ Hz: top figure — barrier with the resonator, bottom figure — classic barrier.

An example of the field structure in the vicinity of the barrier is shown in Fig. 6 (top figure – barrier with the resonator, bottom figure – classical barrier). The figures show a fragment adjacent to the barrier of the spatial distribution of the sound pressure level difference in decibels $\Delta L = 20 \lg(p/p_0)$, here p is the pressure at the observation point in the presence of the barrier, p_0 is the pressure at the observation point in the absence of the barrier. Coordinates are given in meters: 12 m horizontally in front of the barrier and behind the barrier, 12 m up from the ground.

We can clearly see how at the output section of the resonator a domain of reduced pressure is formed. This domain contributes to reducing the noise level penetrating into the shadow zone of the barrier.

4 CONCLUSIONS

1. Based on the PDM, a rigorous solution to the problem of sound scattering on a noise barrier is given. Using the CBP of fields on the boundaries of PD, an effective algorithm for numerical analysis of the sound field in the vicinity of the barrier in the frequency range of interest for practice has been developed.
2. It is shown that the use of the RMS and the CBP of the fields on the boundaries of PD in the problem of sound scattering on the classical barrier gives a good coincidence of the calculated values of the fields for the two options of conjugation of the fields.
3. The CBP of the fields makes it relatively easy to construct a computational algorithm. In this case, increasing the number of nodal points allows you to confidently increase the accuracy of conjugation of sound fields.
4. It is shown that for frequencies above the resonant frequency there is a frequency band in which there is a dip in the frequency response of the integral criterion of the barrier. This indicates the advantage of the barrier with the resonator. As the resonant frequency increases, this frequency band increases. At higher frequencies, the efficiency difference between the traditional barrier and the barrier with a resonator is smoothed out.
5. It is shown that at frequencies below the resonance frequencies there are situations in which the efficiency of the barrier with a resonator is worse than that of the classical barrier.

REFERENCES

- [1] V. GRINCHENKO, I. VOVK, V. MATSYUPURA (2007) "Fundamentals of acoustics". Naukova Dumka. [in Ukrainian].
- [2] V. GRINCHENKO, I. VOVK, V. MATSYUPURA (2018) "Acoustic wave problems". New York: Begell House, Inc.
- [3] B. KOTZEN, C. ENGLISH (2009) "Environmental noise barriers". London/New York: Spon Press.
- [4] L. OSIPOV, V. BOBYLEV, L. BORISOV (2004) "Soundproofing and sound absorption". M.: ST and Astrel [in Russian].
- [5] T. OKUBO, K. YAMAMOTO (2007) Procedures for determining the acoustic efficiency of edge-modified noise barriers. *Applied Acoustics* **68**(7) 797-819.
- [6] K. LI, M. KNOK, M. LAW (2008) A ray model for hard parallel noise barriers in high-rise cities. *J. Acoust. Soc. Amer.* **123**(1) 121-132.
- [7] V. BOROVNIKOV, B. KINBER (1978) "Geometric theory of diffraction". M.: Svyaz [in Russian].

- [8] H. ZIEGELWANGER, M. CONTER, A. FUCHS, P. REITER, R. WEHR (2016) Optimization of an acoustic resonator for noise barrier top elements. Presented at *45th International Congress and Exposition on Noise Control Engineering INTER-NOISE 2016At: Hamburg*.
- [9] N. PAPADAKIS, G. STAVROULAKIS (2020) Finite Element Method for the Estimation of Insertion Loss of Noise Barriers: Comparison with Various Formulae (2D). *Urban Science* **4** 77.
- [10] B. KIM , S. KIM, Y. PARK, M. MIEREMET, H. YANG, J. BAEK, S. CHOI (2021) Development of a Slit-Type Soundproof Panel for a Reduction in Wind Load and Low-Frequency Noise with Helmholtz Resonators. *Applied Science* **11**, 8678.
- [11] S.M.B. FARD, H. PETERS, N. KESSISSOGLU, S. MARBURG (2015) Quasi-periodic noise barrier with Helmholtz resonators for tailored low frequency noise reduction. *Acoustics Hunter Valley*.
- [12] M. MOSER, R. VOLZ (1999) Improvement of sound barriers using headpieces with finite acoustic impedance. *Journal of the Acoustical Society of America* **106** 3049.
- [13] I. URUSOVSKIY (2013) Diffraction of sound on a screen with a fan attachment. *Acoust. Journal* **59**(1) 86-95. [in Russian]
- [14] L. OSIPOV, B. PRUTKOV, I. SHISHKIN, I. KARAGODINA (1975) "Urban planning methods of noise control". M.: Strojizdat [in Russian].